3D joint inversion of geophysical data with Gramian constraints: A case study from the Carrapateena IOCG deposit, South Australia

MICHAEL S. ZHDANOV and ALEXANDER V. GRIBENKO, University of Utah and TechnoImaging
GLENN A. WILSON, TechnoImaging
CHARLES FUNK, OZ Minerals

Explorers are moving to increase the "discovery space" by exploring under cover and to greater depths, e.g., subsalt and sub-basalt exploration for oil and gas, and beneath transported cover for minerals. With this shift, there becomes an increased reliance on geophysical methods to delineate resources with no recognized geological or geochemical expressions. Different geophysical fields provide information about different physical properties of the Earth. Multiple geophysical surveys spanning gravity, magnetic, electromagnetic, and seismic methods are often interpreted to infer geology from models of different physical properties. In many cases, the various geophysical data are complementary, making it natural to consider a formal mathematical framework for their joint inversion to a shared Earth model. There are different approaches to joint inversion. The simplest case of joint inversion is where the physical properties are identical between different geophysical methods (e.g., Jupp and Vozoff, 1975). In other cases, joint inversion may infer theoretical, empirical, or statistical correlations between different physical properties (e.g., Hoversten et al., 2003, 2006). In cases where the physical properties are not correlated but, nevertheless, can be assumed to share a similar structure, joint inversions have been formulated as a minimization of the cross-gradients between different physical properties (e.g., Haber and Oldenburg, 1997; Gallardo and Meju, 2003, 2004). The latter has now been widely adopted by joint inversion practitioners as the de facto standard (e.g., Colombo and De Stefano, 2007; Hu et al., 2009; Jegen et al., 2009; De Stefano et al., 2011).

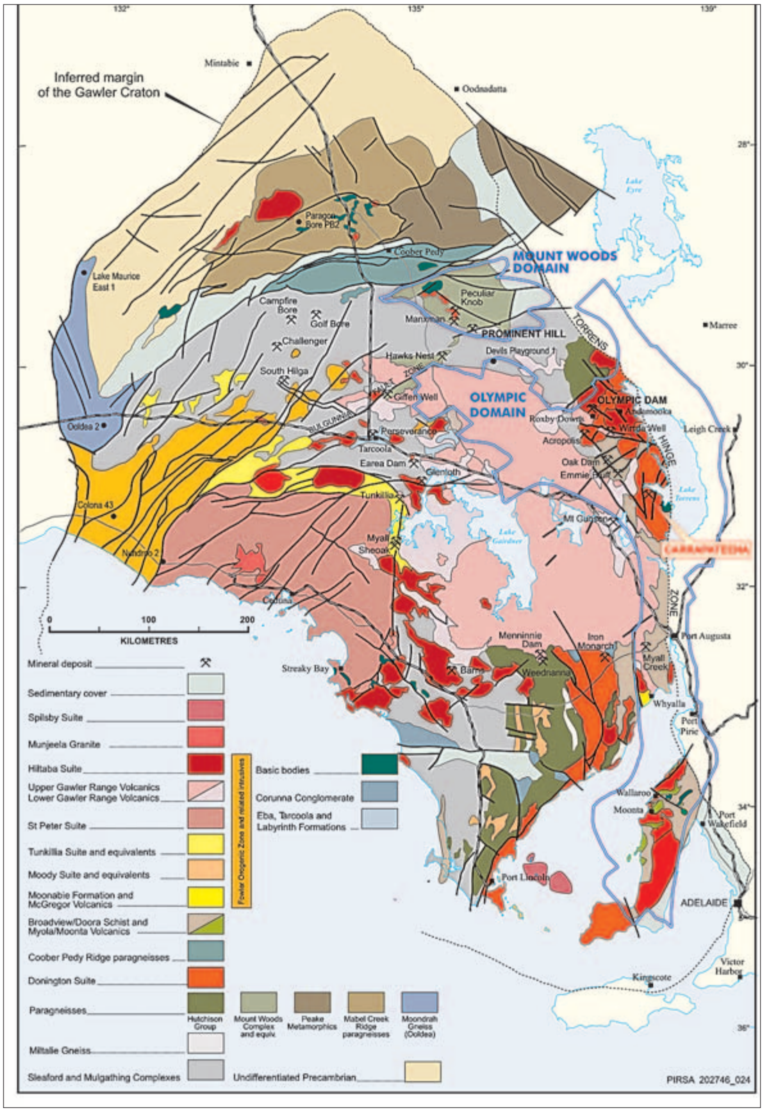

Figure 1. Interpreted geological map of the Gawler Craton, locating the Carrapateena IOCG deposit, Olympic Dam mine, and Prominent Hill IOCG deposits, along with other known, similarly mineralized IOCG systems (after Daly et al., 1998; from Fairclough, 2005).

In practical applications, petrophysical correlations between different physical properties may exist, but their specific forms may be unknown. In addition, there could be correlations between different attributes (transforms or functions) of the model parameters. Following Zhdanov et al. (2012), we address the uncertainty of these correlations by introducing Gramian constraints which are based on the minimization of the determinant of the Gram matrix of a system of the different model parameters or their attributes (i.e., a Gramian). The principle of this approach is that the Gramian provides a measure of correlation between the different model parameters or their attributes. By imposing the additional requirement of the minimum of the Gramian in regularized inversion, we obtain multimodal inverse solutions with enhanced correlations between the different model parameters or their attributes. This approach is general, as it has been shown that extant methods based on petrophysical correlations or crossgradient minimization are special case reductions. However, it is important to note that this method does not require any a priori knowledge about the specific relationships between the different model parameters or their attributes. Here, we apply this method to gravity and magnetic data acquired over the Carrapateena Fe oxide Cu-Au (IOCG) deposit in South Australia, and demonstrate it is possible to interpret lithology and alteration patterns directly from the joint inversion of potential field data.

Regularized joint inversion with Gramian constraints

For regularized joint inversion, we minimize the parametric functional with the Gramian stabilizer:

$$p^a(m^{(1)}, m^{(2)},\ldots,m^{(n)}) = \Sigma_{i=1}^{n}\| A^{(i)}(m^{(1)}) - d^{(i)}\|_D^2 + \alpha c_1 \Sigma_{i=1}^{n} S^{(i)} + ac_2 S_{G_T} \rightarrow min, \quad (1)$$

where, for the i^{th} geophysical method, $A^{(i)}(m^{(i)})$ are the predicted data, $d^{(i)}$ are the observed data, and $S^{(i)}$ are the stabilizing functionals of the corresponding model parameters (Zhdanov, 2002). Following Zhdanov et al. (2012), S_{G_T} is the Gramian stabilizing functional for transformed model parameters:

$$S_{G_T} = \|Tm^{(n)}\|^2_{G_T^{(n)}} = G(Tm^{(1)}, Gm^{(2)},\ldots, Gm^{(n)}). \quad (2)$$

It is implied that the model transform operator, T, may be any function, including the identity operator (for correlations between the model parameters), gradient operator (for structural correlations between the model parameter gradients), or any other operator (e.g., logarithms, Fourier transform, etc.). Note that, according to the properties of the norm $\| \ldots \|^2_{G_T^{(n)}}$ in the Gramian space $G_T^{(n)}$, minimization of the norm enforces correlation between the different transforms (attributes) of the model parameters. The scalars c_1 and c_2 are weighting coefficients which determine the weights of the different stabilizers in the parametric functional. As per classic theory (Tikhonov and Arsenin, 1977), the regularization parameter, α, provides the balance (or bias) between the misfit and stabilizing functionals. At the initial stage of the inversion, coefficients c_1 and c_2 can be selected as unities. After calculating both the stabilizing and Gramian stabilizing functionals and comparing their magnitudes, it could be determined if additional scaling is necessary. The coefficients c_1 and c_2 can be adjusted to bias either stabilizer. To minimize parametric functional 1, we construct a regularized conjugate gradient (RCG) method as per Zhdanov (2002).

Case study: Carrapateena, South Australia

The discovery of the massive Olympic Dam deposit in South Australia's Gawler Craton during 1975 was remarkable not only for the size and grade of the resource, but also for its unpredictable style and geological setting. The geochemical signature had large quantities of Fe oxides (e.g., magnetite, hematite) associated with Cu, Au, Ag, U, Ba, F, and rare earth elements. Since then, the rather broad classification of Fe oxide Cu-Au ("IOCG") deposits has come into general use, and are generally defined as hydrothermal ore systems with strong structural controls and extensive alkali-rich alteration, abundant low-Ti magnetite and/or hematite, economic Cu, Au and minor element resources, and no clear spatial associations with igneous intrusions as per porphyry systems (Williams et al., 2005). Olympic Dam was also a major success for geophysical-led exploration under cover given the deposit's lack of any outcrop (Esdale et al., 2003). The Gawler Craton represents a typical "exploration under cover" scenario where transported cover sequences mask the geological and geochemical expressions of the basement. For targeting IOCG deposits, precompetitive regional gravity and magnetic data sets are publicly available and higher-resolution, proprietary data sets are relatively inexpensive to acquire. The petrophysical properties of IOCG deposits are particularly amendable to potential field data (e.g., Hanneson, 2003), and 3D inversion of gravity and magnetic data has become a routine part of modern exploration workflows (e.g., Williams et al., 2004; Howe, 2009).

The Carrapateena IOCG deposit is in the eastern margin of the Gawler Craton in South Australia, approximately 160 km north of Port Augusta and 100 km southeast of Olympic Dam (Figure 1). The Gawler Craton underlies much of central South Australia, and is defined as a region of Archaean-to-Mesoproterozoic crystalline basement comprising metasediments, volcanics, and granites that have not undergone substantial deformation since 1450 Ma (Thomson, 1975; Daly et al. 1998). The eastern margin of the Gawler Craton is defined by the Torrens Hinge Zone, a zone of Neoproterozoic rifting initiated during the development of the Adelaidian Basin (Ferris et al., 2002). Overlying the northeastern edge of the Gawler Craton is the Stuart Shelf, which consists of incomplete sequences of flat-lying Neoproterozoic sediments such as the outcropping Arcoona Quartzite, Corraberra Sandstone, Woomera Shale, and variably gritty siltstones to sandstones, with minor interbeds of dolomite. A basal conglomerate marks the unconformity between these sediments and the older crystalline basement.

Following its discovery in 2005 by RMG Services under the South Australian Government's Plan for Accelerated Exploration (PACE) (Fairclough, 2005), Carrapateena was extensively explored by joint venture partner Teck Australia and was demonstrated to have strong similarities with the nearby Olympic Dam IOCG deposit, albeit at a smaller scale (Vella and Cawood, 2006, 2012). Carrapateena lies at the intersection of an interpreted major NNE-trending structure and the northwest-trending fault corridor, both of which are thought to have played a role in focusing mineralization at Olympic Dam. As Carrapateena lies beneath approximately 470 m of Stuart Shelf sediments, geophysical surveys played an important role in both the discovery and delineation of the deposit. Yet, relative to other Gawler Craton IOCG deposits, limited information has been published about Carrapateena. Fairclough (2005) discussed the regional geological setting and discovery history. Vella and Carwood (2006) provided a preliminary description of the local geological and geophysical setting. A revision by Vella and Carwood (2012) included subsequent petrophysical measurements (Vella and Emerson, 2009, 2012), as well as gravity, induced polarization (IP), resistivity, magnetotelluric (MT), and downhole electromagnetic (EM) surveys and interpretations.

At Carrapateena, the mineralization is hosted within the Carrapateena Breccia Complex, occurring in a hematite-silica-sericite-mineralized sequence of breccia, with clasts and fragments or granite, gneiss, and vein-quartz (Figure 2). The host rock is variably foliated and/or sheared gneissic quartz granite and quartz diorite which has been dated at 1857 ± 6 Ma (Vella and Emerson, 2009), assigning it to the Donington Suite. The basement rocks are locally intruded by felsic and mafic dikes. Alteration minerals are mainly hematite, chlorite, and sericite, with locally abundant silica and carbonate (siderite and/or ankerite). Accessory minerals include barite, monazite, anatase, magnetite, apatite, fluorite, and zircon. Copper sulfide mineralization comprises chalcopyrite; bornite; rare covelite and rare chalcocite, mainly as disseminations, blebs; and veinlets. Pyrite is locally abundant. Drilling returned some spectacular intercepts. For example, CAR050 intersected 905 m at 2.1% Cu and 1 g/t Au. In April 2011, OZ Minerals purchased Carrapateena from Teck Australia, and soon afterwards released an inferred resource for the southern portion of the deposit of 203 Mt at 1.31% Cu, 0.56 g/t Au, 270 ppm U3O8, and 6 g/t Ag (OZ Minerals, 2011a, 2011b).

In 2005, Fugro Airborne Surveys acquired total magnetic intensity (TMI) and radiometric data over the deposit on east-west flight lines spaced 200 m apart, with a nominal ground clearance of 50 m. The Carrapateena deposit lies on the southwestern margin of a broad magnetic anomaly of moderate amplitude, and is

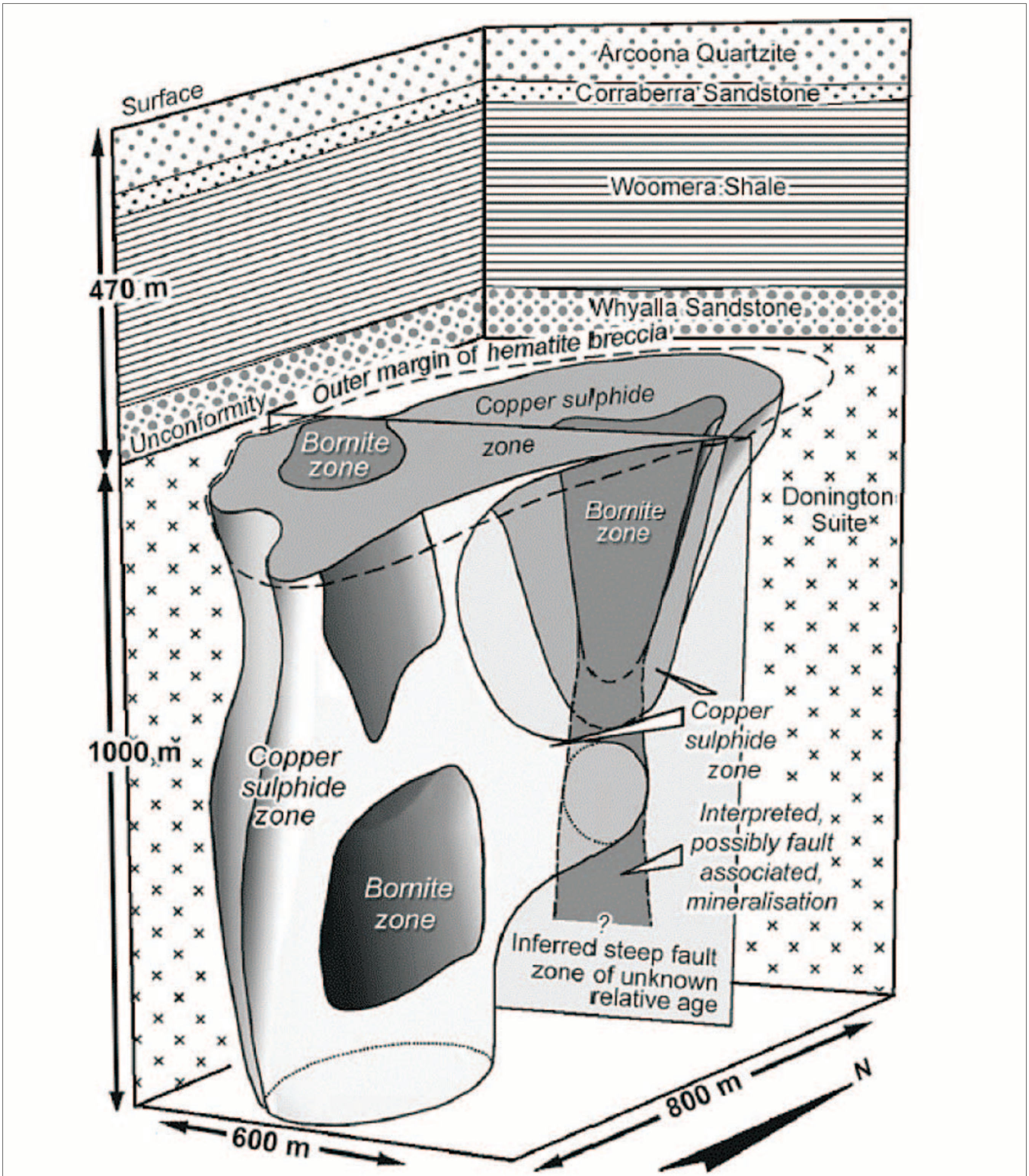

Figure 2. *Cartoon of the geology of the Carrapateena IOCG deposit, located beneath Stuart Shelf sediments (courtesy of PIRSA).*

associated with a weak, discrete, ellipsoidal magnetic response, being elongated in a north-south direction and having an amplitude of approximately 200 nT. Three separate ground-based gravity surveys were acquired over the deposit. In 1996, Dynamic Satellite Surveys acquired 204 gravity stations on a 500 × 500-m grid. In 2003, MIM Exploration acquired 207 gravity stations on a 400 × 400-m grid. In 2006, Haines Surveys acquired data on a 200 × 200-m grid. The Carrapateena deposit is characterized by a weak (2.5 mGal) gravity high that is near-coincident with the observed magnetic response. Laboratory-based physical property measurements were undertaken on 72 drill core samples (Vella and Emerson, 2009). The cover sequences generally exhibit low densities and susceptibilities. Basement rock densities increase with increasing hematite and/or magnetite and/or sulfide content. As expected, basement susceptibilities correlate with magnetite content.

We jointly inverted the gravity and magnetic data over Carrapateena. Given the low densities of the cover sequences, the 2.67 g/cc Bouguer reduction density was not appropriate. A stratified density model was constructed from the known cover sequence depths and densities (Vella and Emerson, 2009), with the correction then applied to the 2.67 g/cc Bouguer gravity data. The regional background trend was also removed from the TMI data. The depth to basement, a surface approximately 470 m below the surface, was used to constrain the upper boundary of the 3D Earth models. The 3D Earth model was discretized into 1,152,000 cells of 100 × 100 × 25 m dimension. The kernels and depth weightings used for modeling and inverting the gravity and TMI responses are described by Čuma et al. (2012). No a priori models were used for either the density or the susceptibility. We applied our Gramian constraints on the physical properties themselves, with no other a priori information or constraints enforced. Our choice of Gramian constraints is appropriate, given the petrophysical relations that are known to exist between the different physical properties of IOCG deposits (e.g., Hanneson, 2003). However, note that the advantage of the Gramian approach is that it does not require a priori knowledge about the specific relationships between the different physical properties. We also applied focusing regularization (Zhdanov, 2002). Initially, coefficients c_1 and c_2 in Equation 1 were selected as unities. After scaling each of the density and susceptibility models by their maximum value, both the stabilizing and Gramian stabilizing functionals had comparable magnitudes, and no additional scaling was necessary. An adaptive regularization scheme was

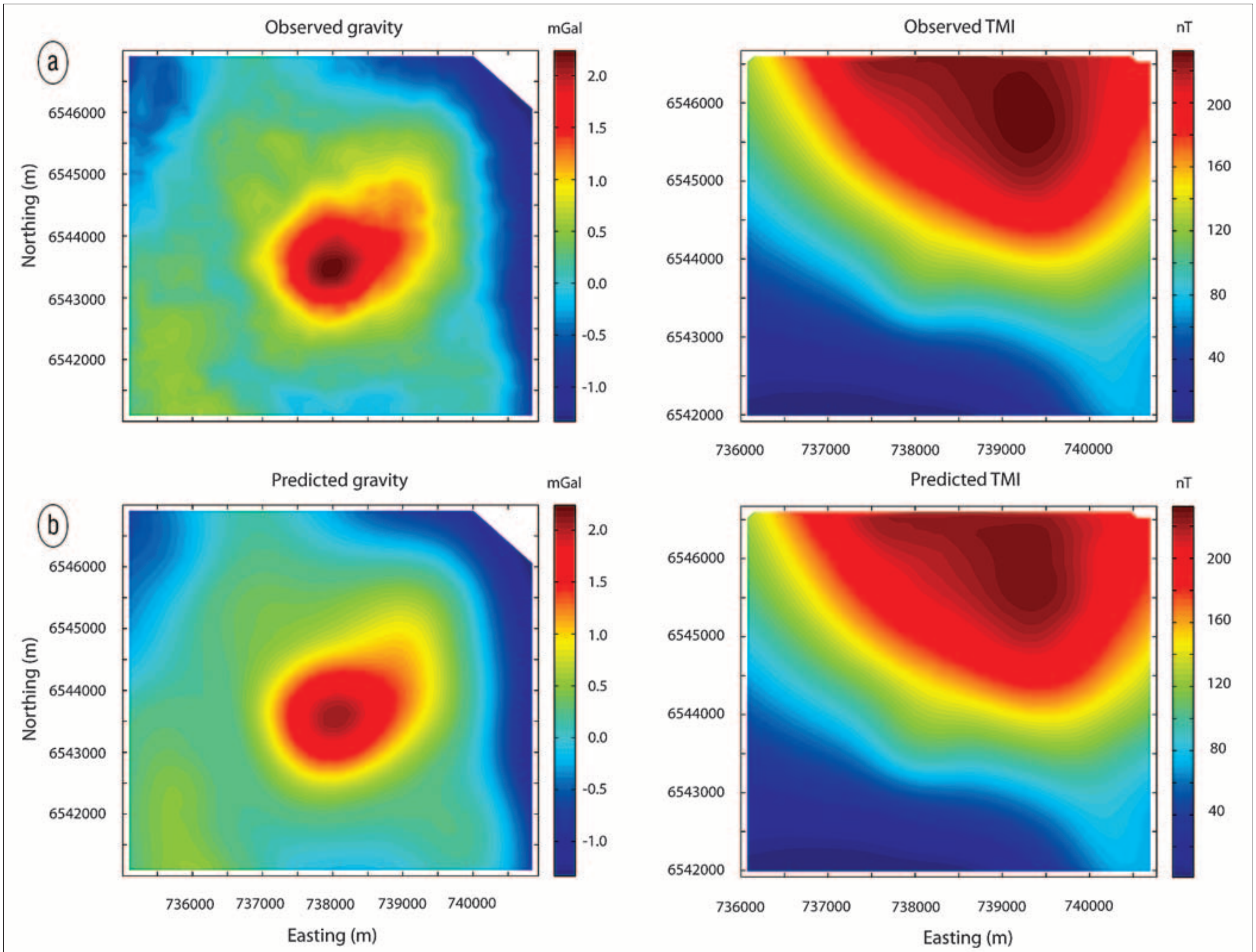

Figure 3. Observed (a) and predicted (b) surface-based gravity (left panels) and airborne TMI (right panels) from the 3D joint inversion of the Carrapateena IOCG deposit. The weighted misfit between observed and predicted data is less than 2%.

used with the initial regularization parameter calculated as the ratio of the norm of the residual functional to the norm of the stabilizing functionals, and a relaxation ratio of 0.9. The inversion converged to less than 2% weighted misfit (Figure 3).

We crossplotted the recovered densities and susceptibilities for all cells in the earth model, along with the laboratory-derived densities and susceptibilities for drill core from Vella and Emerson (2009) (Figure 4). As expected, there is a continuum of the recovered physical properties. However, we note that the physical properties recovered from the joint inversion coincide with the actual physical properties. As shown in Figure 4, we are able to categorize the physical properties into four discrete lithological groups based on the physical properties. Group 1 is characterized by high densities, and includes HMX (>90% hematite, <10% granite breccia), HMXH (60–90% hematite, 10–40% granite breccia), HMXH + py (pyrite-bearing), HMXH + Cu (copper-bearing), GRXL + Cu (40–70% granite, 30–60% hematite breccia; copper-bearing), GRLX + bn (bornite-bearing), and GRXH + Cu (70–90% granite, 10–30% hematite breccia; copper-bearing). Group 2 is characterized by intermediate densities, and includes GRXL, and GRXL + cpy (chalcopyrite-bearing). Groups 1 and 2 collectively represent the Carrapateena Breccia Complex. Group 3 is characterized by low density and low susceptibility, and includes the Donnington suite host. The overburden sequences share the same physical properties but have been classed as the separate Group 5. Group 4 is characterized by low density and high susceptibility, and includes the Donnington suite host.

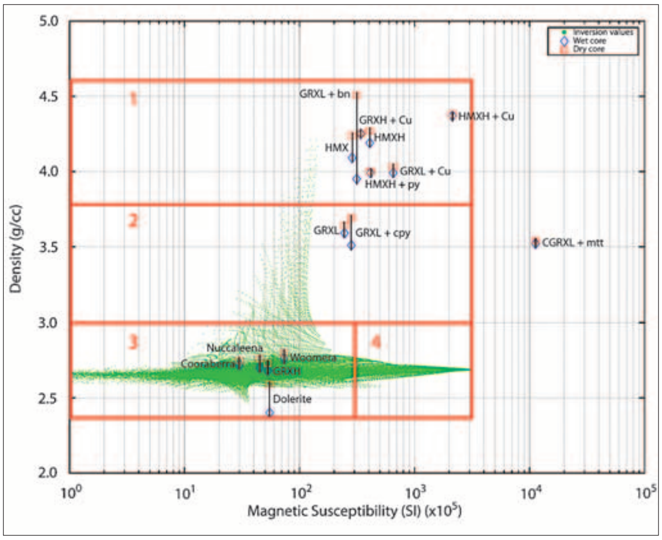

Figure 4. *Crossplot of the density and susceptibility values for all cells in the 3D Earth model (green dots) as recovered from joint inversion superimposed on the laboratory-based density and susceptibility measurements of drill core samples from Vella and Emerson (2009). The abbreviations for different lithologies are consistent with Vella and Emerson (2009). Groups have been assigned on the basis of their physical properties.*

We are able to assign a lithological group to each cell in the model. Figure 5 presents the vertical cross-section of such a lithological model through the Carrapateena deposit along 6543500 N. Note that we are able to recover a core of Group 1 lithologies surrounded by a halo of Group 2 lithologies. This reflects the most strongly hematite ± copper sulfide mineralized zone of the deposit surrounded by a halo of less hematite altered, less brecciated lithologies (c.f., Figure 2). The Donnington suite host is characterized by Group 3 and 4 lithologies, and the Stuart Shelf cover sequences characterized by Group 5 lithologies. We note that additional geological information could constrain the inversion further. However, for the purpose of initially mapping alteration ahead of more detailed targeting, we have demonstrated that joint inversion of potential field data can add significant geological insight.

Conclusions

The interpretation of geology from geophysical data represents a data fusion problem as different geophysical fields provide information about different physical properties of the Earth. In many cases, the various geophysical data are complementary and self-constraining, making it natural to consider a formal mathematical framework for their joint inversion to a shared earth model. By introducing Gramian spaces of model parameters and Gramian constraints, we have developed a generalized method of joint inversion for multimodal geophysical data that

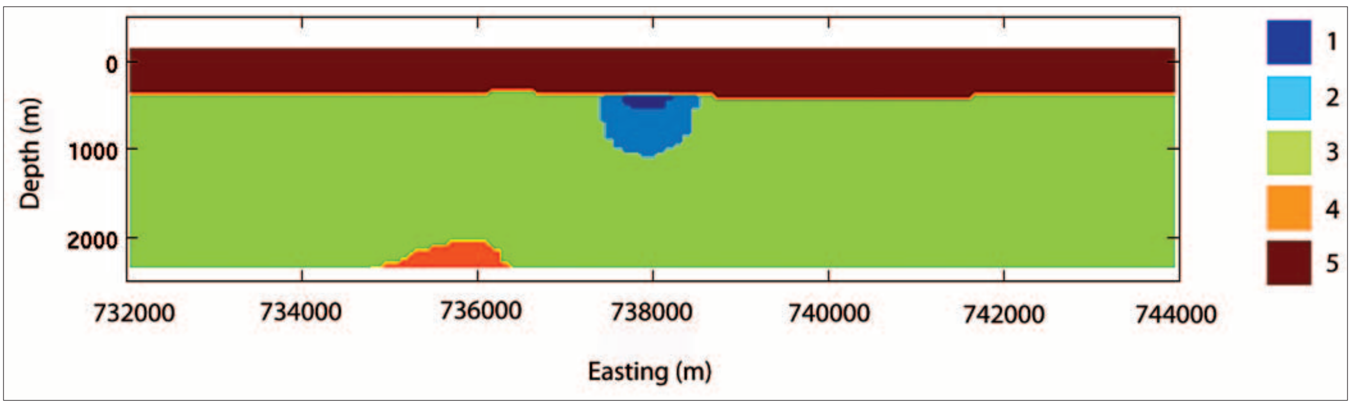

Figure 5. *Vertical cross-section along 6543500 N for the lithological classification (Figure 4) of density and susceptibility values recovered from the 3D joint inversion of gravity and magnetic data. The Carrapateena deposit is located at approximately 738000 E. Group 1 is characterized by high density and represents the most strongly hematite ± copper sulfide mineralized core of the deposit. Group 2 is characterized by moderate density, and represents the less intensely brecciated and hematized halo of the deposit. Group 3 is characterized by low density and low susceptibility, and represents the host. Group 4 is characterized by low density and high susceptibility, and also represents the host. Group 5 is characterized by low density and low susceptibility, and represents the cover sequence.*

encompasses existing methods of petrophysical or structural constraints as special case reductions. Importantly, the method assumes a correlation between the different model parameters or their attributes exists, but the specific forms are unknown. Our case study for joint inversion of gravity and magnetic data from the Carrapateena IOCG deposit demonstrates the efficacy of the method for mineral exploration under cover—in particular, for the mapping of lithology (alteration) directly from potential field data. The joint inversion method extends to other geophysical data (e.g., magnetotellurics, seismic) and this is the subject of ongoing activities. TLE

References

Colombo, D. and M. De Stefano, 2007, Geophysical modeling via simultaneous joint inversion of seismic, gravity, and electromagnetic data: Application to prestack depth imaging: The Leading Edge, **26**, no. 3, 326–331, http://dx.doi.org/10.1190/1.2715057.

Čuma, M., G. A. Wilson, and M. S. Zhdanov, 2012, Large-scale 3D inversion of potential field data: Geophysical Prospecting, **60**, http://dx.doi.org/10.1111/j.1365-2478.2011.01052.x.

Daly, S. J., C. M. Fanning, and M. C. Fairclough, 1998, Tectonic evolution and exploration potential of the western Gawler Craton: AGSO Journal of Australian Geology and Geophysics, **17**, 145–168.

De Stefano, M., F. G. Andreasi, S. Re, M. Virgilio, and F. F. Snyder, 2011, Multiple-domain, simultaneous joint inversion of geophysical data with application to subsalt imaging: Geophysics, **76**, R69–R80.

Esdale, D., D. F. Pridmore, J. Coggon, P. Muir, P. Williams, and F. Fritz, 2003, The Olympic Dam copper-uranium-gold-silver-rare earth element deposit, South Australia: A geophysical case history, in M. Dentith (ed.), Geophysical Signatures of South Australian Mineral Deposits, Centre for Global Metallogeny, The University of Western Australia, Perth, Publication **31**, 147–168.

Fairclough, M., 2005, Geological and metallogenic setting of the Carrapateena Fe-O-Cu-Au prospect—A PACE success story: Mesa Journal, **38**, 4–7.

Ferris, G. M., M. P. Schwarz, and P. Heithersay, 2002, The geological framework, distribution, and controls of Fe-oxide and related mineralization in the Gawler Craton, South Australia, Part 1: Geological and tectonic framework, in T. M. Porter, ed., Hydrothermal iron oxide copper-gold and related deposits: PGC Publishing, Adelaide, 1–23.

Gallardo, L. A. and M. A. Meju, 2003, Characterization of heterogeneous near-surface materials by joint 2D inversion of DC resistivity and seismic data: Geophysical Research Letters, **30**, no. 13, 1658–1661, http://dx.doi.org/10.1029/2003GL017370.

Gallardo, L. A. and M. A. Meju, 2004, Joint two-dimensional DC resistivity and seismic travel-time inversion with cross-gradients constraints: Journal of Geophysical Research, **109**, B3, B03311, http://dx.doi.org/10.1029/2003JB002716.

Haber, E. and D. Oldenburg, 1997, Joint inversion: A structural approach: Inverse Problems, **13**, no. 1, 63–67, http://dx.doi.org/10.1088/0266-5611/13/1/006.

Hanneson, J. E., 2003, On the use of magnetics and gravity to discriminate between gabbro and iron-rich ore-forming systems: Exploration Geophysics, **34**, no. 2, 110–113, http://dx.doi.org/10.1071/EG03110.

Hoversten, G. M., R. Gritto, J. Washbournez, and T. Daley, 2003, Pressure and fluid saturation prediction in a multicomponent reservoir using combined seismic and electromagnetic imaging: Geophysics, **68**, 1580–1591.

Hoversten, G. M., F. Cassassuce, E. Gasperikova, G. A. Newman, J. Chen, Y. Rubin, Z. Hou, and D. Vasco, 2006, Direct reservoir parameter estimation using joint inversion of marine seismic AVA and CSEM data: Geophysics, **71**, no. 3, C1–C13, http://dx.doi.org/10.1190/1.2194510.

Howe, B. R., 2009, Constrained potential field inversions in areas under cover: Examples from Gawler Craton IOCG prospects: Presented at 20th ASEG Geophysical Conference and Exhibition, Adelaide.

Hu, W. Y., A. Abubakar, and T. M. Habashy, 2009, Joint electromagnetic and seismic inversion using structural constraints: Geophysics, **74**, no. 6, R99–R109, http://dx.doi.org/10.1190/1.3246586.

Jegen, M. D., R. W. Hobbs, P. Tarits, and A. Chave, 2009, Joint inversion of marine magnetotelluric and gravity data incorporating seismic constraints: Preliminary results of sub-basalt imaging off the Faroe Shelf: Earth and Planetary Science Letters, **282**, no. 1–4, 47–55, http://dx.doi.org/10.1016/j.epsl.2009.02.018.

Jupp, D. L. B. and K. Vozoff, 1975, Joint inversion of geophysical data: Geophysical Journal of the Royal Astronomical Society, **42**, 977–991.

OZ Minerals Ltd., 2011a, OZ Minerals acquires Carrapateena copper project: ASX Release, 9 March 2011. www.ozminerals.com. Accessed September 2012.

OZ Minerals Ltd., 2011b, Carrapateena Mineral Resources Statement, 14 April 2011. www.ozminerals.com. Accessed September 2012.

Thomson, B. P., 1975, Gawler Craton South Australia, in C. L. Knight, ed., Economic geology of Australia and Papua New Guinea, Australasian Institute of Mining and Metallurgy, 461–466.

Tikhonov, A. N. and V. Y. Arsenin, 1977, Solution of ill-posed problems: Winston and Sons.

Vella, L. and M. Cawood, 2006, Carrapateena: Discovery of an Olympic Dam-style deposit: Preview, no. 122, 26–30.

Vella, L. and M. Cawood, 2012, Geophysical characteristics of the Carrapateena iron-oxide copper-gold deposit: Presented at 22nd ASEG Geophysical Conference and Exhibition.

Vella, L. and D. Emerson, 2009, Carrapateena: Physical properties of a new iron-oxide copper-gold deposit: Presented at 20th ASEG Geophysical Conference and Exhibition.

Vella, L. and D. Emerson, 2012, Electrical properties of magnetite- and hematite-rich rocks and ores: Presented at 22nd ASEG Geophysical Conference and Exhibition.

Williams, N. C., R. Lane, and P. Lyons, 2004, Towards 3D maps of alteration under cover: Regional constrained 3D inversion of potential field data from the Olympic Cu-Au province, South Australia: Presented at 17th ASEG Geophysical Conference and Exhibition, Sydney.

Williams, P. J., M. D. Barton, D. A. Johnson, L. Fontbote, A. de Haller, G. Mark, N. H. S. Oliver, and R. Marschik, 2005, Iron oxide copper-gold deposits: Geology, space-time distribution, and possible modes of origin: Economic Geology, 100th Anniversary Volume, 371–405.

Zhdanov, M. S., 2002, Geophysical inverse theory and regularization problems: Elsevier.

Zhdanov, M. S., A. V. Gribenko, and G. A. Wilson, 2012, Generalized joint inversion of multimodal geophysical data using Gramian constraints: Geophysical Research Letters, **39**, no. 9, L09301, http://dx.doi.org/10.1029/2012GL051233.

Acknowledgments: The authors acknowledge TechnoImaging and OZ Minerals for support of this research and permission to publish. M. S. Zhdanov and A. V. Gribenko acknowledge support from the University of Utah's Consortium for Electromagnetic Modeling and Inversion (CEMI).

Corresponding author: glenn@technoimaging.com